JOURNAL OF QUATERNARY SCIENCE (2021) **36**(5) 934–945 ISSN 0267-8179. DOI: 10.1002/jqs.3273

JQS Journal of Quaternary Science QRA Quaternary Research Association

Exploring the extent to which fluctuations in ice-rafted debris reflect mass changes in the source ice sheet: a model–observation comparison using the last British–Irish Ice Sheet

DAVID J. WILTON,[1] GRANT R. BIGG,[2]* JAMES D. SCOURSE,[1] JEREMY C. ELY[2] and CHRIS D. CLARK[2]
[1]Department of Geography, University of Exeter, Penryn, Cornwall, UK
[2]Department of Geography, University of Sheffield, Sheffield, UK

Received 24 June 2020; Revised 27 November 2020; Accepted 11 January 2021

ABSTRACT: The British and Irish Ice Sheet (BIIS) was highly dynamic during the Late Quaternary, with considerable regional differences in the timing and extent of its change. This was reflected in equally variable offshore ice-rafted debris (IRD) records. Here we reconcile these two records using the FRUGAL intermediate complexity iceberg–climate model, with varying BIIS catchment-level iceberg fluxes, to simulate change in IRD origin and magnitude along the western European margin at 1000-year time steps during the height of the last BIIS glaciation (31–6 ka BP). This modelled IRD variability is compared with existing IRD records from the deep ocean at five cores along this margin. There is general agreement of the temporal and spatial IRD variability between observations and model through this period. The Porcupine Bank off northwestern Ireland was confirmed by the modelling as a major dividing line between sites possessing exclusively northern or southern source regions for offshore IRD. During Heinrich events 1 and 2, the cores show evidence of a proportion of North American IRD, more particularly to the south of the British Isles. Modelling supports this southern bias for likely Heinrich impact, but also suggests North American IRD will only reach the British margin in unusual circumstances.

KEYWORDS: British and Irish Ice Sheet; coupled model; deglaciation; Heinrich event; ice-rafted debris

Introduction

An ice sheet with a large marine component, such as the West Antarctic Ice Sheet today, is suspected to be dynamic, with major change occurring quickly but not spatially synchronously, leading to major consequences for iceberg flux rates, ocean circulation and, potentially, sea level (Hughes, 1975; MacAyeal, 1992; Bamber *et al.*, 2009; Thomas, 2014). The best studied past analogue for such a dynamic marine glacial system is the British and Irish Ice Sheet (BIIS) of the last glacial period (Clark *et al.*, 2018). The evolution, and particularly retreat pattern, of the last glacial BIIS has been studied from both a largely 'deep ocean' perspective, driven by temporal and spatial distributions in along-margin ice-rafted debris (IRD) flux, sea surface temperature (SST) and lithology (e.g. Scourse *et al.*, 2009); and a largely 'terrestrial and shelf' perspective, driven by the spatial and temporal distribution of glaciogenic landforms (e.g. Clark *et al.*, 2012, 2020). Both of these approaches lead to the conclusion that the BIIS was indeed dynamic in terms of the asynchronous nature of the peak advance and retreat patterns. However, what is currently lacking in the literature for any past ice sheet, is a formal reconciliation of the detailed reconstruction of these two perspectives.

Our approach to this reconciliation is to use the well-constrained BRITICE-CHRONO reconstruction of the growth and retreat of the British–Irish Ice Sheet during the last glacial (31 to 15 ka BP) to compute potential iceberg discharges into the ocean (Clark *et al.*, 2020). To track the transport and deposition of the resulting IRD we use an intermediate complexity coupled iceberg–climate model (Levine and Bigg, 2008) to make IRD predictions across this time period, accounting for temporal climate and ice sheet change. These model ice sheet–iceberg–ocean predictions are then compared with the empirical record of IRD at five well-described locations. Put differently, the novelty here is that we use iceberg trajectory modelling to permit exploration and reconciliation of the regional ice sheet and IRD records. To our knowledge this is the first time such an approach has been undertaken; the significance being that a large body of literature (e.g. Hemming, 2004; Peck *et al.*, 2007; Hall *et al.*, 2011) implicitly assumes that there is a tight, predictable and easily interpreted relationship between ice mass change and IRD occurrence. We aim to assess how simple or complex this relationship is using a well-constrained ice sheet with a rich IRD record.

The BIIS context for this analysis is first described, followed by a discussion of the various IRD and iceberg flux data, as well as the climate model to be used. A simulation of the evolution of the combined flux and iceberg distribution, using 1000-year time slices from 31 to 16 ka BP is then presented (the ice sheet had disappeared by 15 ka BP). The sensitivity of the simulation to both Heinrich event intervention from the western Atlantic, and two different reconstructions for the ice flux from the Porcupine Bank, off western Ireland, is then tested. The paper concludes with a discussion of the results and consideration of the consequences for the terrestrially focused reconstruction.

*Correspondence: G. R. Bigg, as above.
E-mail: grant.bigg@sheffield.ac.uk

BIIS context

We focus our investigation within the BIIS context around a series of questions to gain insights into the interactions:

1. Does IRD typically come from the obvious local source, as suggested by Scourse *et al.* (2009), or do ocean currents confuse the picture?
2. To what extent can icebergs originating from other ice sheets affect regional records?
3. Do IRD events in the marine record reflect mean iceberg fluxes, or mostly record advance or retreat phases?
4. To what extent are the core sites in, rather than avoiding, iceberg alleys, and is this a significant factor that should be acknowledged in making IRD interpretations?
5. Do variations in ocean currents and the position of the North Atlantic Polar Front (NAPF) over time either directly or indirectly affect the transport of icebergs?

The investigation is driven by the west European offshore IRD perspective epitomised by Scourse *et al.* (2009) and the comprehensive BIIS palaeo-ice sheet reconstruction from the BRITICE-CHRONO project (http://www.britice-chrono.group.shef.ac.uk/; reported in Clark *et al.*, 2020). The reconstructed palaeo-ice stream routes from BRITICE-CHRONO are shown in Fig. 1, along with the IRD marine core positions. Note that ice streams internal to the continental shelf, as well as from the independent Shetland ice mass, are not considered in our investigation.

The open ocean IRD perspective of the late BIIS evolution appears to be simplified by the vast majority of the offshore IRD originating from the BIIS itself, where IRD lithologies can be fingerprinted (Peck *et al.*, 2007; Scourse *et al.*, 2009). The main possible contaminant of IRD from the Laurentide Ice Sheet (LIS) of North America is only found in the marine record along a small part of the central west European margin, off southwest Ireland, for short intervals, during Heinrich events (Fig. 2; Scourse *et al.*, 2009). It is possible that IRD sourced from Greenland, Iceland or the Faroes has been conflated with BIIS-sourced IRD in this analysis. However, the observed lack of LIS material off the glacial British Isles is consistent with the possible trajectories from the iceberg modelling work of Bigg *et al.* (2010). The first two questions above are driven by these findings from Scourse *et al.* (2009). One major question raised by their IRD analysis was the indicative meaning of IRD: does an increase in IRD flux represent an extension in the calving margin during ice sheet growth, or rapid collapse during deglaciation, or both (Question 3 above)?

Questions 4 and 5 above are driven by how one expects the marine IRD record to be driven by changes in climate, and associated changes in the geography of ice sheet extent and thickness. One argument is that the BIIS will expand or reorientate southwards during colder stadials, resulting in IRD expanding in the southern shelf region as more ice is calved to the south, while the IRD record north of the Polar Front will experience a period of constant IRD flux during these southward excursions (Scourse *et al.*, 2009). During our period of interest there are Greenland interstadials at ~23 (GIS2), 27 (GIS3) and 28.5 (GIS4) ka BP (Rasmussen *et al.*, 2014). The combination of this hypothesised mechanism and the IRD record of Fig. 2 led Scourse *et al.* (2009) to suggest early, major advance of shelf ice off western Scotland after GIS4, being maintained until around GIS2. A major southward expansion of ice is consistent with the stadial between GIS2 and GIS3, with the central shelf around Porcupine Bank maintaining significant IRD flux throughout, being near or north of the NAPF throughout much of the period.

The terrestrial and shelf-centred view of the evolution of the peak and retreat of the BIIS, based on Clark *et al.* (2012), updated and consolidated by Clark *et al.* (2020) in a much-enhanced data-rich and ice sheet modelling analysis, starts from evidence that the BIIS had a significant ice core within northern Britain and Ireland

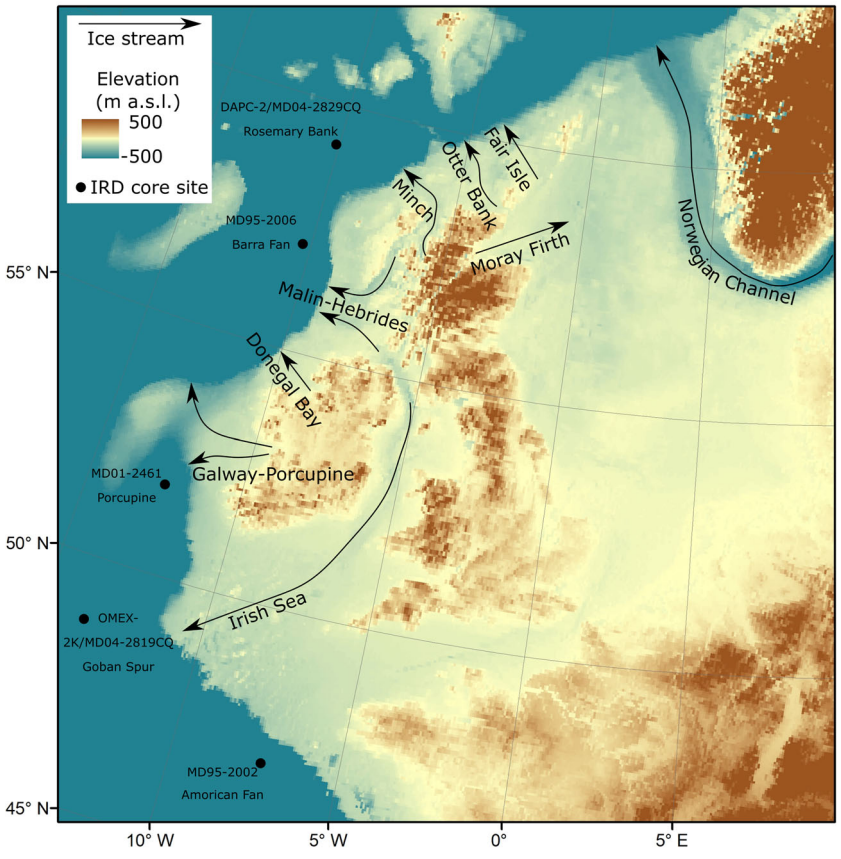

Figure 1. Map showing the study area of the British Isles, with the ice-rafted debris cores used in Scourse *et al.* (2009), and the main ice streams from the BRITICE-CHRONO reconstruction of Clark *et al.* (2020). The topography is taken from Weatherall *et al.* (2015). [Color figure can be viewed at wileyonlinelibrary.com]

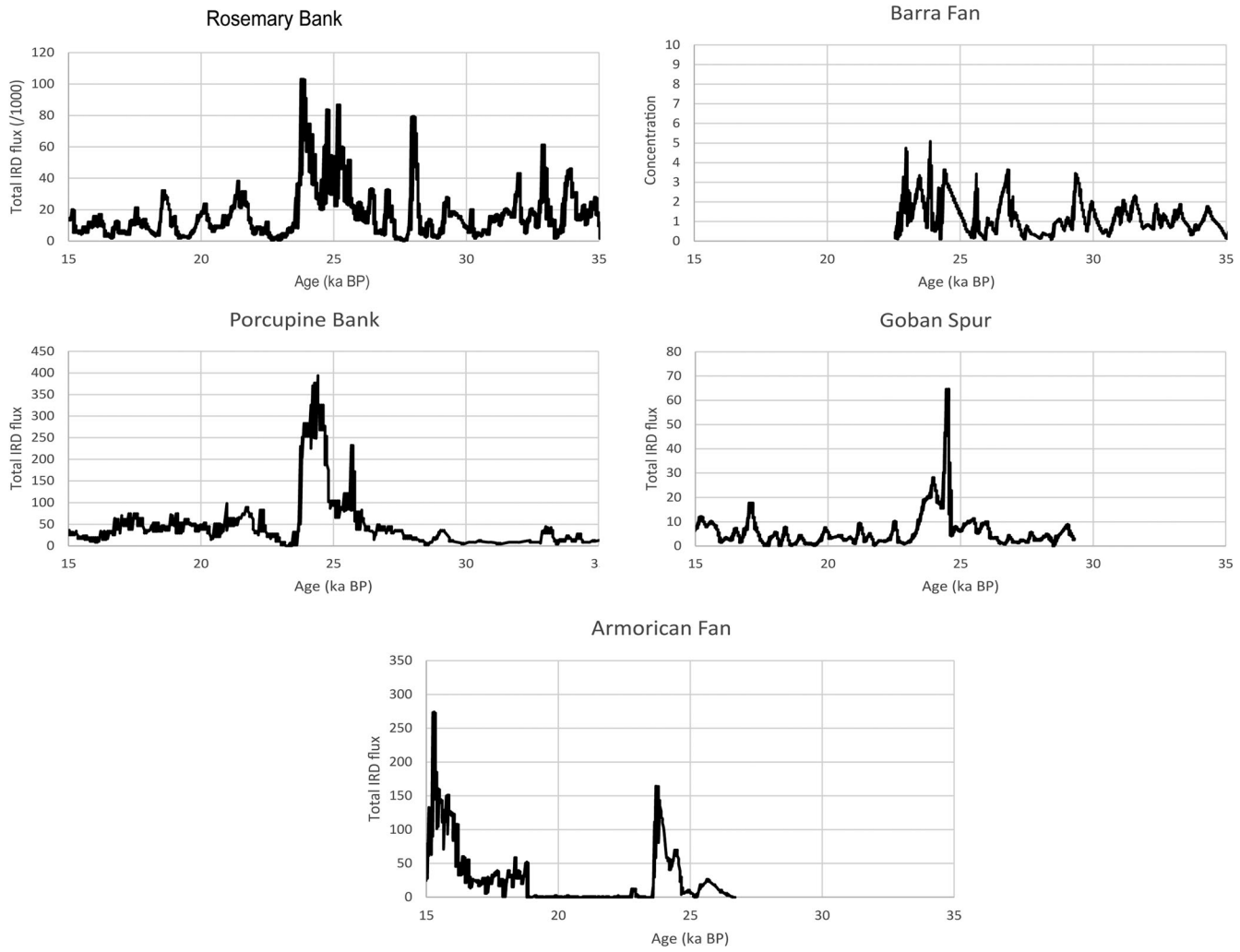

Figure 2. Ice-rafted debris flux ((>150 μm grains cm^{-2} kyr^{-1})/1000) over 35–15 ka BP, in cores shown in Fig. 1, from Scourse *et al.* (2009). Note, however, that Barra Fan shows the concentration, rather than flux, with units >250 μm grains g^{-1} (see text for discussion). Cores shown from north to south (when reading left to right, top to bottom; see Table 1 for core names and positions). Note that the timing of H1 ~15–16 ka BP, H2 ~24–25 ka BP and H3 is ~30–31 ka BP.

around 30 ka BP, but not extending across the North Sea or into southern Ireland. A rapid and major ice sheet expansion is thought to have occurred around 27 ka BP, with ice extending out to the continental shelf edge around much of western Britain and Ireland (Peters *et al.*, 2016; Callard *et al.*, 2018). This is reconstructed to be short-lived, with significant retreat from the western Scottish shelf, around the time of, or just after, GIS3 (Ó Cofaigh *et al.*, 2019). This was followed by another period of rapid expansion (25–24 ka BP), although at this time centred in the Irish Sea and extending towards the Isles of Scilly (Smedley *et al.*, 2017; Scourse *et al.*, 2019). This advance is reconstructed to be short-lived also, but the ice extent, and calving fluxes, from the core BIIS remained similar for several thousand years. It was then not until after 20 ka BP that the main BIIS began to retreat back onshore, shrinking gradually back to its Scottish core by 16 ka BP.

The reasons for both of these reconstructions given above are partially ascribed to climate change; for example, through high relative sea level (Ó Cofaigh *et al.*, 2019), but also to internal ice stream dynamics (e.g. Sejrup *et al.*, 2016; Gandy *et al.*, 2018). Here, through use of an intermediate complexity climate and iceberg model (Levine and Bigg, 2008), the linkage between the two perspectives is studied by attempting to reconcile the temporal and spatial variability of both the iceberg calving flux and the offshore IRD flux. As part of this reconciliation the question about the sensitivity of the marine core locations will also be addressed; this is Question 4 as posed earlier.

Data and method

IRD data

The main IRD data which this paper uses are described in Scourse *et al.* (2009) and Table 1. There are five cores spanning the west European shelf from northwest Scotland to Brittany. The core locations are shown in Fig. 1, and the IRD data in Fig. 2. As shown in Table 1, the various cores cover different age limits, but here interest is restricted to 31–16 ka BP. Note that we only use core MD04-2829CQ (Hall *et al.*, 2011) from Rosemary Bank and not the other in this location discussed in Scourse *et al.* 2009, namely DAPC-2, as the latter does not cover the full extent of the time period under consideration.

As can be seen from Table 1, the cores have varying sedimentation rates so age models for all cores are based on tuning the percentage frequency of the >150 μm fraction of polar planktonic foraminfer *Neogloboquadrina pachyderma* sinistral (Nps) to the GISP2 ice core $\delta^{18}O$ record (Scourse *et al.*, 2009). The rationale for this tuning is that the %Nps is a proxy for the meridional movement of the NAPF, and so linked to northern Atlantic climate variability, as will be the Greenland ice sheet's properties. A number of ^{14}C and tephra ages help constrain these records (for more details, see Scourse *et al.* (2009) and papers referenced therein). The one exception to this procedure is core MD95-2006, from the Barra Fan. While prior to c. 30 ka BP the sedimentation at this core seems largely hemipelagic, and so a

Table 1. Key data for ice-rafted debris cores.

Core	Location	Position	Water depth (m)	Core type	Length (cm)	Age span (ka)
1 MD04-2829CQ	Rosemary Bank	58.95°N, 9.57°W	1743	GBC	1007	c. 41
2 MD95-2006	Barra Fan	57.03°N, 10.06°W	2120	GPC	3000	c. 60
3 MD01-2461	Porcupine Seabight	51.08°N, 12.92°W	1153	GPC	2002	>130
4 OMEX-2K	Goban Spur	49.09°N, 13.43°W	3658	Kasten	254	30
5 MD95-2002	Armorican Fan	47.45°N, 8.45°W	2174	GPC	2990	>113

GBC = CASQ giant box coring system; GPC = CALYPSO giant piston coring system.

tuning approach can be used (but for the >250 μm fraction), after c. 30 ka BP the location of this core on an active trough mouth fan led to considerable turbiditic sedimentation in its record (Knutz *et al.*, 2001). This makes interpretation of the details of the IRD record more difficult. There are some ^{14}C dates in this section to help constrain the age model (Knutz *et al.*, 2001); these agree with the reconstructions presented in the next section. The Barra Fan IRD record is therefore discussed here, but requires care in its interpretation.

For interpretation of the IRD record it is important to note that provenance analysis carried out in Scourse *et al.* (2009), and papers referenced therein for specific cores, showed that most of the IRD record comes from locally sourced lithic material (see Peck *et al.* (2007) for more details). This is likely to have been largely carried by icebergs derived from the catchment areas of adjacent ice streams. While it is very difficult to discriminate IRD derived from a marginal sea-ice source as opposed to that transported by icebergs (St. John *et al.*, 2015), the former is unlikely to be widespread along the eastern Atlantic margin and will not be transported far before melting (Vettoretti and Peltier, 2013). The only long-distance transport of non-BIIS IRD found in Scourse *et al.* (2009) was limited material carried from the LIS during Heinrich events, specifically H1 and H2 in our time period. This is only present in significant quantities at those times in the Goban Spur core, with a marginal H2 signal in the Porcupine Bank core. Note that the absence of LIS dolomitic carbon around H3, at 30 ka BP, is consistent with this event originating from a different, possibly Arctic, ice sheet (Bigg *et al.*, 2011).

Ice volume calculations

To estimate the ice flux from the BIIS between 31 and 16 ka BP, steady-state ice sheet simulations forced to coincide with the reconstructed isochrones of Clark *et al.* (2020) were performed at 1000-year intervals. Ice thickness was derived using an ice sheet model which assumes perfectly plastic ice flow (Gowan *et al.*, 2016). This plastic ice sheet model requires three inputs: ice extent, basal shear stress and basal topography. Ice extent was prescribed to the plastic ice sheet model from the reconstruction of Clark *et al.* (2020). Basal shear stress was assigned according to glacial geomorphological units using the map of Gandy *et al.* (2018). The general bathymetric chart of the oceans (www.gebco.net; Weatherall *et al.*, 2015) was used as an input basal topography. All simulations had a horizontal resolution of 5 km.

A balance flux approach, whereby the flux of ice at a point is assumed to balance upstream accumulation, was used to estimate ice flux through the major outlets of the BIIS (Le Brocq *et al.*, 2006). The balance flux approach has been shown to reasonably recreate the ice flux patterns of the Antarctic ice sheet (Le Brocq *et al.*, 2006). The balance flux algorithm requires inputs of ice thickness (derived from the plastic ice sheet model) and accumulation. Unfortunately, we do not have an accumulation proxy or climate–ice sheet model which is consistent with the reconstruction of Clark *et al.* (2020). Therefore, variation in latitudinal and longitudinal gradients of accumulation were assumed to be the same as for contemporary precipitation, an approach which has been shown to be successful for modelling aspects of the BIIS (Patton *et al.*, 2016). Ice flux was then integrated from the balance flux calculations across the margin of each of the major BIIS outlets and the Norwegian Channel Ice Stream (Fig. 1). The volume of ice in each catchment was calculated for every time interval. Changes in volume (either a growth during ice advance, or reduction during ice retreat) were distributed to adjacent time steps to correct for ice volume storage or loss in the final estimates of iceberg flux, as shown in Fig. 3. Though both the plastic model and balance flux algorithm contain large simplifications of the mechanics of ice sheet flow and palaeoclimatic conditions, the derived iceberg fluxes are of a similar order of magnitude to previous estimates (Bigg *et al.*, 2010) and provide a first-order estimate of the importance of different catchments for iceberg flux through

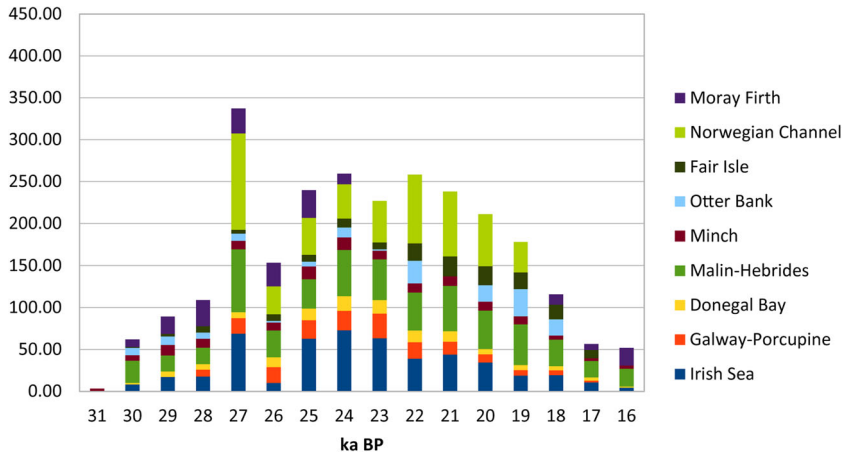

Figure 3. Reconstructed iceberg fluxes over 31–16 ka BP from main ice streams around the BIIS, including the Norwegian Channel. Calculated using volume changes per catchment. Units: km^3 yr^{-1}. [Color figure can be viewed at wileyonlinelibrary.com]

time (Fig. 3). These simple models match the reconstructed ice limits and deglaciation chronology of the BIIS in a manner that more complex models may struggle to achieve.

FRUGAL intermediate complexity model

The FRUGAL (Fine ResolUtion Greenland And Labrador) intermediate complexity global climate model includes coupling between ocean, radiative–advective atmospheric, simple advective–thermodynamic sea-ice and iceberg trajectory models (Levine and Bigg, 2008). FRUGAL has been used in a number of palaeoclimate studies over a range of times including the last glacial period (Levine and Bigg, 2008; Bigg *et al.*, 2010, 2011), the penultimate glaciation (Green *et al.*, 2010) and the Early Pleistocene (Rea *et al.*, 2018). The model uses a curvilinear grid with the North Pole in Greenland, giving an enhanced resolution in the Arctic and North Atlantic (Wadley and Bigg, 2000). Here we use a fine resolution grid of 182 ×211 cells, which is equivalent to approximately 2° longitude by 1.5° latitude in the Southern Hemisphere, but with a resolution of 20 km around the Greenland coast. The details of the ocean and sea-ice model configuration are given in the similar resolution, but present-day, study by Wilton *et al.* (2015). The atmospheric part of FRUGAL is a simple radiative–advective atmosphere (Fanning and Weaver, 1996) that allows for advection of water vapour. All the simulations discussed in this paper use a monthly varying glacial wind stress, which has no feedback from the SST field (Levine and Bigg, 2008). The basic topography and bathymetry of the model is as described in the last glacial FRUGAL simulations (e.g. Levine and Bigg, 2008), but with minor modifications around the British Isles to reflect knowledge of ice sheet extent (Clark *et al.*, 2012), and taking into account the finer resolution of the model grid in the shaping of local bathymetry for important gateways and shallow seas. The iceberg module has both dynamic and thermodynamic components, although in this study there is no feedback between the iceberg model and the rest of the FRUGAL system. The dynamical processes included in the iceberg model are ocean/atmosphere/sea-ice drags, the Coriolis force, pressure gradients in the surrounding ocean, and wave radiation. The main thermodynamic processes represented are basal melting, buoyant convection, wave erosion, and several smaller terms due to sublimation and latent heat transfer. Icebergs may roll over (Wagner *et al.*, 2017) and grounded icebergs are allowed to melt instantaneously (Levine and Bigg, 2008). Model icebergs are divided into 10 different size classes, ranging from 0.491 to 492×10^9 kg in mass, based on observations of present-day Arctic and Southern Ocean icebergs, excluding giant icebergs. Each model berg is assigned a scale factor appropriate to that size of berg from its specific seed site. Summing the mass of each berg, multiplied by its scale factor, gives the average ice discharge per quarter year expected from that seed site (see Levine and Bigg (2008) for a depiction of this in the last glacial period).

A 1000-year spin-up simulation was run, using orbital parameter and atmospheric CO_2 levels from 21 ka BP (as in Levine and Bigg (2008)). By the end of this simulation all large-scale ocean and atmospheric fields had reached an essential state of equilibrium. A set of sensitivity experiments were then carried out. In this set, 16 × 10 year simulations were carried out, with each simulation using a different orbital parameter configuration with steps of 1000 years in the parameters, as determined from the equations in Berger (1988), from 31 ka BP to 16 ka BP. The climate changes for each step, being due to minor changes in eccentricity, obliquity and precession (Fig. S1), are small and the equilibrium state has shifted smoothly within a few years (Fig. S2). Tests where atmospheric CO_2 was changed similarly with time, in line with ice core changes (Lüthi *et al.*, 2008), showed minimal difference across the time period studied. In the set of 10-year simulations the volume change iceberg flux (Fig. 3) is seeded around the British Isles, with iceberg fluxes elsewhere globally, including around the North Atlantic, as given in Levine and Bigg (2008).

A sensitivity study to investigate the local impact of adjustment to iceberg release sites to take account of different scenarios for ice extent around the Porcupine Bank (Peters *et al.*, 2016) was also carried out. To investigate fully the impact of Heinrich events on the possible supply of LIS IRD to the British margin, 10-year simulations starting from year 5900 of the St. Lawrence and Hudson Strait Heinrich event studies of Levine and Bigg (2008) were run, but including giant icebergs of 20 and 40 km in length in the iceberg seed file, replacing the two largest iceberg classes of the original scheme, but preserving total iceberg flux. The intention of this test was to address Question 2 by ascertaining whether icebergs more typical of those released from LIS ice sheet collapse would reach further east before melting.

Results

Ocean properties

While there are minor changes in the global ocean and atmospheric properties between each simulation across the set of 16 time slices, from 31 to 16 ka BP (Table S1), the key features of North Atlantic Ocean currents and SST remain the same. The typical 30 m ocean current is shown in Fig. 4, with an expanded view for the northeast Atlantic off western Europe shown for a selection of time slices in Fig. S3. The basic ocean circulation consists of a sub-tropical gyre, separating from the

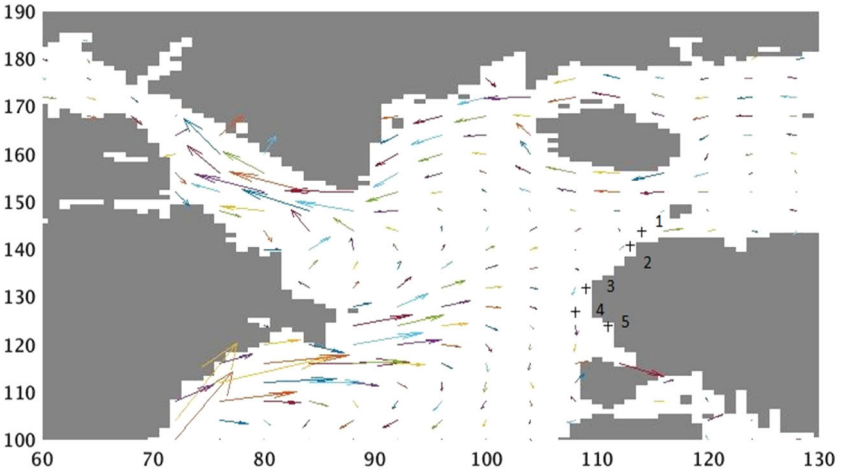

Figure 4. The mean 30 m depth ocean current over the last two years of the simulation is shown for the 26 ka BP time slice. The five ice-rafted debris core sites are shown by '+', and numbered as in Table 1. Note, the land boundaries are on the model grid. Arrow length is linearly related to speed, with longest, off eastern North America, ~30 cms^{-1}. [Color figure can be viewed at wileyonlinelibrary.com]

North American coast off New England, and sub-polar gyres in the northwestern Atlantic and Norwegian–Greenland Sea. Note that the five IRD sites, whose positions are marked on Fig. 4, are well placed to capture IRD in the coastal currents off glacial Britain, and to show north–south movement of the NAPF boundary. This boundary, separating the southward return flow of the sub-tropical gyre from the northward flow along the British Isles entering the sub-polar gyre systems, occurs north of Ireland, near the Donegal and Malin–Hebrides ice streams (Fig. 1). This is the case for all time slices (Fig. S3), although the similarity is a reflection of the wind stress being the same in all time slices, even if temperatures and salinities differ because of the orbital parameter variation. The Greenland–Norwegian Sea sub-polar gyre is driven by a European coastal shelf current, with the western outflow being both through the Denmark Strait, but also southeast of Iceland. The northwestern Atlantic sub-polar gyre is centred in the Labrador Sea, but there is a general weak, northwestward circulation in much of the northern Atlantic (Figs. 4 and S3). Note that this tends to be weakest offshore from the BIIS, a feature that we will return to in the discussion.

Iceberg distributions

The simulated iceberg density field across the northern Atlantic is shown in Fig. 5 for a selection of time slices, to illustrate the impact of the temporal evolution of BIIS iceberg fluxes (Fig. 3). Note that the seeded iceberg flux from all other ice sources outside the BIIS is fixed for all time slices, and what is shown is the average density for the last two years of a 10-year iceberg run, to ensure the simulation's near-surface properties have reached equilibrium with each change in orbital parameters across the set. The variation in Fig. 5 is therefore from a mix of forced BIIS iceberg release changes, changes in iceberg trajectories and lifetimes due to simulation-dependent ocean temperature and currents, and random noise due to the two-year data window.

At 31 ka BP, the earliest time slice shown in Fig. 5, the only source of BIIS icebergs is from the Minch Ice Stream (Fig. 3), so there are very few icebergs present off the British Isles. The simulations overall show that icebergs from other, non-BIIS, sources are rare and only appear at a few time slices, and exclusively from Scandinavia. At the IRD sites, undetectable levels of IRD are found for this time slice (Fig. 6), consistent with Fig. 5. The low iceberg density area off northwestern Iberia comes from North American icebergs; this is clearer in later time slices.

By 27 ka BP the BIIS had expanded significantly in all directions, with marine ice spreading out to the continental shelf edge around much of western Britain and Ireland (Fig. 3). This led to icebergs being calved into the ocean extensively, but in the model they tend to be trapped in the near-shelf area (Fig. 5), with transport southwards towards Iberia and northwards into the Norwegian Sea, but few spreading westward into the Atlantic proper. The model suggests there is a strong source separation for the icebergs that feed the IRD sources, with those cores north of the NAPF being supplied largely from the Malin–Hebrides ice stream, while those south of the NAPF are fed from the Porcupine Bank, and further south (the Armorican Fan), from the Irish Sea (Fig. 6).

Over the next few thousand years, while the iceberg flux stabilises and calving retreats from the continental shelf edge in places, the basic modelled iceberg distribution, both in spread (Fig. 5) and direction (Fig. 6), remains similar. It is only after 21 ka BP that the retreat of the BIIS from its marine margins intensifies, so that by the end of our study period, 16 ka BP, only iceberg calving off Moray Firth and the Malin–Hebrides ice stream continues in the north, with a very limited Irish Sea flux, leaving only a patchy iceberg distribution around the British Isles (Fig. 5). Note that the source regions of IRD remain essentially the same, with only the northernmost two locations retaining modelled IRD signatures by 16 ka BP (from Malin–Hebrides; Fig. 6).

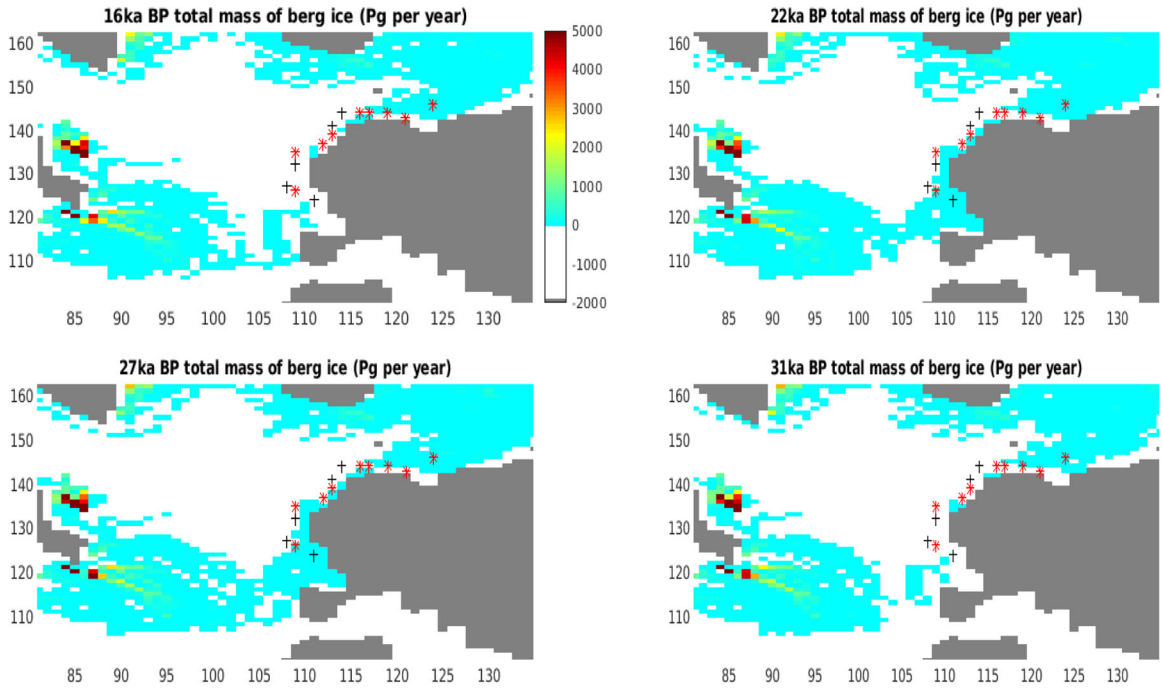

Figure 5. Iceberg total mass density maps, averaged for the last two years of four time-slice simulations: 16, 22, 27 and 31 ka BP. The BIIS fluxes, seeded from the red '+' sites, vary over time as given in Fig. 3. The ice-rafted debris core sites are shown as black '+'. Note, the land boundaries are on the model grid. The iceberg density is scaled by 10^{12} kg yr^{-1}, with the maximum capped at 5000. [Color figure can be viewed at wileyonlinelibrary.com]

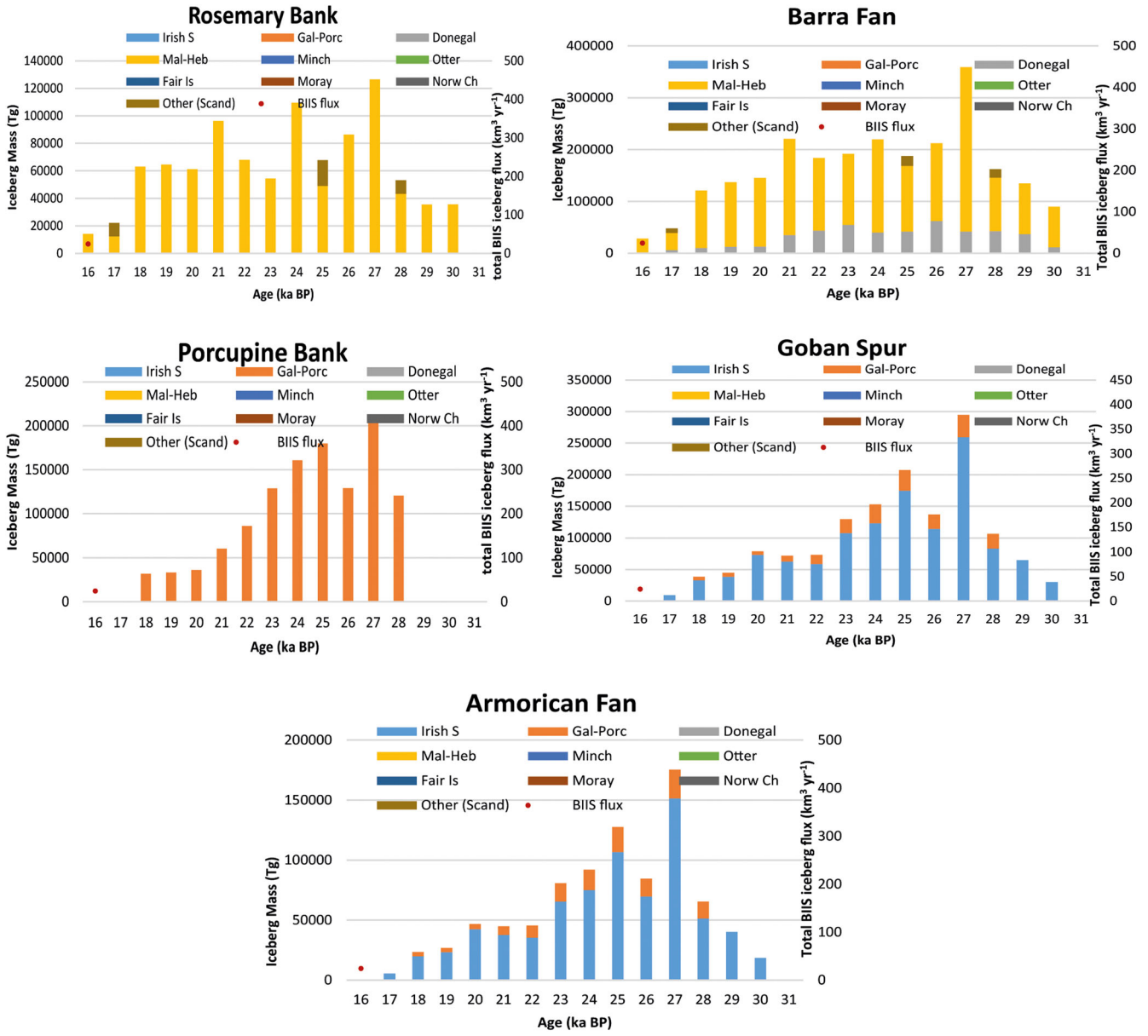

Figure 6. Bar charts of the ice-rafted debris (IRD) source variation over time within 2° of the 5 IRD marine cores, using modelled iceberg mass (in Tg) as a proxy (see Table 1 for core names and locations). Note that the dotted line is the total BIIS iceberg flux (in km^3 yr^{-1}; see right-hand scale), as reconstructed in Fig. 3. See Figs. 1 and 3 for release sites and fluxes, respectively. [Color figure can be viewed at wileyonlinelibrary.com]

Sensitivity tests

Two sensitivity tests were carried out to test hypotheses about alternative iceberg sources. Firstly, there is some argument over the extent of the ice bridge out to Porcupine Bank during the peak glacial period (Peters *et al.*, 2016). Did the ice extend all the way to Porcupine Bank, essentially leading to a northern and southern calving source from the resulting ice bridge, or was there a less extensive, single source ice stream in the area? Simulations were therefore re-run, with the Galway Porcupine iceberg flux split equally between a northern and southern seed site (Fig. 7). To better simulate the rapid retreat of the Irish Sea Ice Stream the Irish Sea seed point was also moved towards the coast (except at 26 ka BP; Fig. 7). As with the previous runs, no Galway Porcupine icebergs moved north, and the overwhelmingly dominant source of icebergs from Galway Porcupine south was from the southern release site. Only a very few northern Galway Porcupine source icebergs contributed to the Porcupine Bank and Armorican Fan IRD sites (Fig. S4).

The other sensitivity run involved testing the hypothesis that production of giant icebergs from a Heinrich event collapse of the LIS would enable some LIS bergs to survive the trans-Atlantic crossing. We have already seen that modelling ordinary icebergs leaving the LIS means they do not reach the British Isles (Fig. 4). Using a Heinrich event simulation, where ocean conditions are modified by the much larger LIS iceberg flux of a Heinrich event (Levine and Bigg, 2008), and running simulations with both ordinary and giant icebergs forming part of the flotilla entering the Atlantic, means that a few icebergs, in both cases, are modelled to reach southern Britain (Fig. 8).

Discussion

Comparison of model and IRD data

The temporal resolution of the IRD record in the five cores is variable, and the model simulations are only for each 1000 years

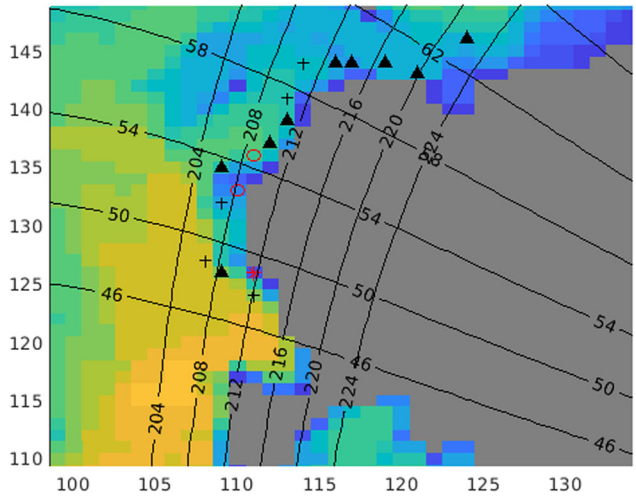

Figure 7. Changes to model iceberg seed points off the Porcupine Bank and Irish Sea, for local ice margin sensitivity studies. The main iceberg release sites are shown by ▲, while the Galway Porcupine split sites are shown by O and the Irish Sea modified site by ∗. The ice-rafted debris marine cores are shown by '+'. The offshore shading shows the local model ocean depth, in model levels; the grey area shows the land grid. Latitude circles (46–62°) and longitude lines (204–224°; reduce by 220 to get values relative to Greenwich meridian) shown for orientation. [Color figure can be viewed at wileyonlinelibrary.com]

between 31 and 16 ka BP. The units of the two iceberg measures are also different. The cores record IRD in grains cm^{-2} kyr^{-1}, in a size range (grains g^{-1} in the case of Barra Fan; see Fig. 2), while the model results give the mass of icebergs found within 2° of a core site over a two-year period (Fig. 6). For each core, Fig. 9 therefore shows both records averaged over 1000 years across 31–16 ka BP, with the respective units on opposite *y*-axes. It is the correlation of the two sets of data, and particularly the timing of major respective peaks, that is of interest. Both IRD sourcing by Scourse *et al.* (2009) and the identification of iceberg origin by the model suggest local sourcing of the majority of material, with northward movement north of the Porcupine Bank and southward movement from here and south of this area throughout the whole period. Thus Fig. 9 shows that, for the BIIS, Question 1 is answered in the affirmative, with local sources dominating the IRD deposition. This is also found to be the case in other areas close to past ice sheets, such as the Denmark Strait (Andrews *et al.*, 2014) and the Labrador Sea (Pearce *et al.*, 2015). However, IRD is well known to be able to travel a very long way in the right oceanographic situations (e.g. Becquey and Gersonde, 2002; Hemming, 2004; Bigg *et al.*, 2010).

A key question for this paper (Question 3) is to what extent the IRD fluxes represent balance ice flux, advance or retreat phases of the ice sheet providing the IRD. The iceberg–climate model was forced by assumed balance ice fluxes. At each core site the Fig. 9 comparison shows that the model captures the peak IRD flux around 25–27 ka BP, although in some places with a 1000-year mismatch, perhaps reflecting the resolution of the ice-sheet reconstruction. However, the details of the comparison vary. These will be examined in turn, from north to south, starting with Rosemary Bank (see Fig. 2 for the detailed IRD record and Fig. 9 for the smoothed comparison). Here the IRD observations show the presence of IRD throughout the period of interest, with a sharp peak around 28 ka BP, followed by a more prolonged peak ~24–25.5 ka BP. The iceberg model also shows significant background levels of IRD throughout, but with one peak, around 27 ka BP. This peak occurs because of the strong peak in local catchment balance at this time (Clark *et al.*, 2020). Past reconstruction has suggested a rapid retreat from the continental edge, but then stabilisation (Clark *et al.*, 2012, 2020) inshore. It is possible that the later (24–25 ka BP) observed IRD peak is associated with the collapse of the shelf-edge extension of the BIIS, rather than reflecting a period of peak expansion of the ice sheet. This has been hypothesised for other areas (Andreassen *et al.*, 2014) and is a classic interpretation of Heinrich event IRD peaks (Hemming, 2004). Such rapid retreat would be smoothed out over the 1000-year time steps of the ice stream flux model and so not be seen as an abrupt step in the iceberg model forcing.

Barra Fan is the next site south. This core only has an IRD record until c. 22 ka BP because of the strongly turbiditic nature of the sediments. However, prior to this time there is excellent agreement in the timing of the peaks in both IRD flux and modelled iceberg number, and some similarity in magnitudes, with the earlier peak being reduced relative to the two later peaks. The fairly continuous ice-streaming activity suggested by Callard *et al.* (2018) is borne out by both model and IRD observations. The mid-margin core at Porcupine Bank showed one main peak in both IRD and iceberg model data. The iceberg peak is ~1000 years later than the IRD peak, but this difference may be due to the details of the core age model or the ice sheet-wide reconstruction. Again, both suggest a period of flux build-up for a few thousand years prior to the peak, from an initially low level. The modelled iceberg number (Fig. 9) is maintained at a higher level for longer after the peak than is the case for the IRD signal. The rapid decline and then re-establishment of IRD levels after the 24–25 ka BP peak (Fig. 2) suggests that the actual ice sheet can respond very rapidly (Peters *et al.*, 2016); faster than the time stepping of either the model or ice flux calculations permit.

The penultimate core in this sequence is Goban Spur, off southwestern Ireland. Both model and IRD observations suggest a persistent low background level of iceberg presence here, with both possessing one major peak. The actual (IRD)

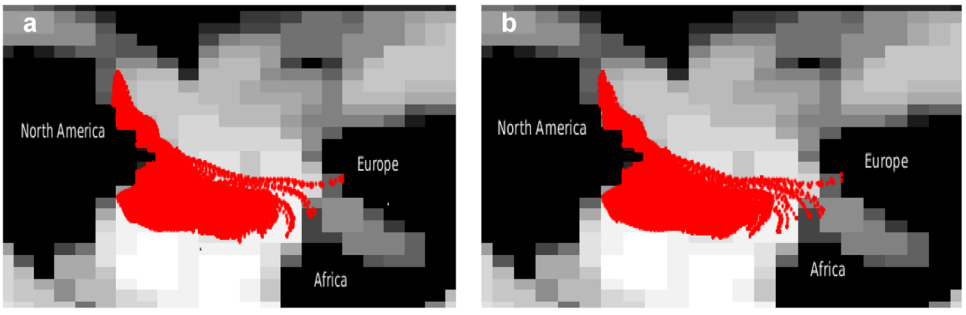

Figure 8. The impact of iceberg size on the trajectory pattern of icebergs released from the LIS, a) standard berg sizes, b) giant icebergs. The plots are from model runs of 10 years' duration, with dotted red lines showing trajectories. A handful of icebergs get close to the Goban Spur and Armorican Fan core sites in both cases. Background ocean shading shows model ocean depth, in grid levels. [Color figure can be viewed at wileyonlinelibrary.com]

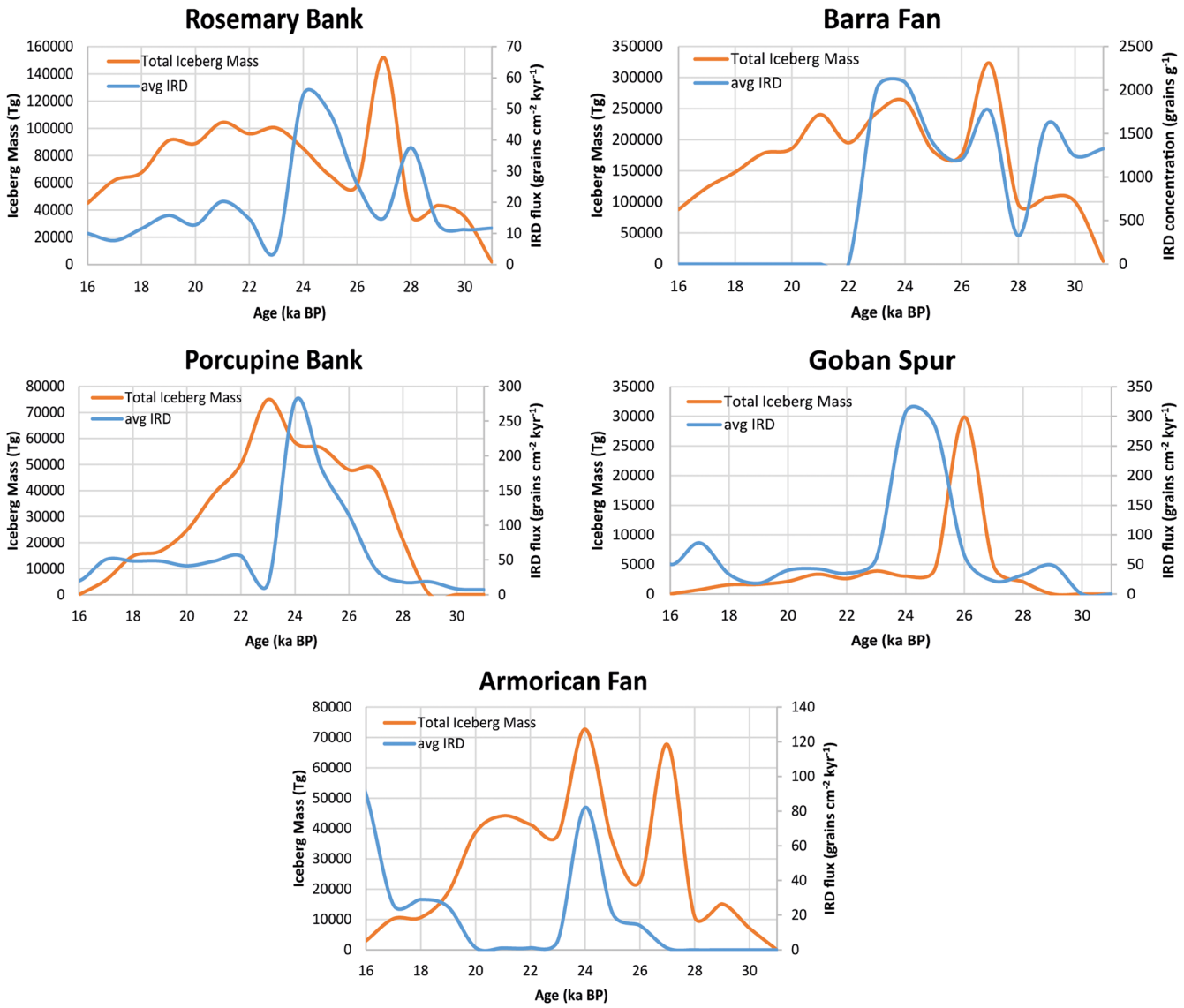

Figure 9. Comparison of the observed ice-rafted debris flux (blue; in >150 μm grains cm^{-2} kyr^{-1})/1000, except for Barra Fan, where units are >250 μm grains g^{-1}) with the modelled iceberg mass flux (orange; Tg within 2° of the core site, over years 9–10 of the simulation) at the five core sites (see Fig. 1). Note, both records have been smoothed with a 1000-year averaging, for comparability. Cores shown from north to south (when reading left to right, top to bottom; see Table 1 for core names and positions). [Color figure can be viewed at wileyonlinelibrary.com]

peak occurs 1–2000 years after that in the iceberg model. Given the sharp timing of the Irish Sea extension in the balance flux calculations (Fig. 3), yet the lack of an early IRD peak either at the Goban Spur, or on the Armorican Fan around 27 ka BP, suggests that the reconstructions of peak extent around 25 ka BP (Ballantyne *et al.*, 2017; Scourse *et al.*, 2019) are more consistent with the IRD record. The final core IRD record, at the Armorican Fan, has both notable similarities and differences with the modelled iceberg fluxes. The lack of an observed 27 ka BP peak has already been mentioned. However, both records capture a peak around 24 ka BP, as the Celtic Sea advance rapidly retreated (Scourse *et al.*, 2019). Both show some IRD more recently in the record, but the modelled fluxes are much greater. A likely reason for this difference is because the ocean and iceberg model coastline does not alter during the return of the Celtic and Irish Seas (Fig. 7), meaning the model releases icebergs too far out to sea after ~25 ka BP. Model icebergs thus reach the Armorican Fan from the Irish Sea (see Fig. 6) when in reality they either had much further to travel, thus melting, or were grounded within the contemporary shallow water of the Irish and Celtic Seas.

From consideration of each of the IRD records, and comparison with the iceberg–climate model's iceberg density, it is clear that the answer to Question 3 is that, while prolonged ice stability and so slowly evolving balance ice fluxes lead to a sustained marine IRD record, peaks in this record relate strongly to change, being particularly sensitive to rapid retreat. Nevertheless, rapid advance can also lead to IRD peaks in circumstances where the advance allows icebergs to enter the open ocean.

The influence of the LIS in the British margin IRD record

It is clear from the provenance analysis of the IRD in the five cores examined here that the only periods of notable presence of sediment from the LIS are during Heinrich events 1 and 2 (Scourse *et al.*, 2009). Even during those major climatic events, LIS material is only found on the Goban Spur and at very small levels on the Porcupine Bank; the latter mostly during H2. This agrees with the iceberg model results. During 'normal' periods, as shown in Fig. 5, modelled icebergs from the LIS may just

reach the Iberian margin at low concentrations, but they do not penetrate further north. The prevailing surface currents act against any northward movement along the European margin north of Iberia (Fig. 4), preventing LIS icebergs reaching the British margin. However, during Heinrich events, the cooling of the climate and ocean, combined with the impact of a colder, fresher North Atlantic on the ocean currents (Levine and Bigg, 2008), means that some icebergs can penetrate to the European margin off southwestern Ireland (Fig. 8). These do not have to be giant icebergs from an ice shelf collapse, but the presence of such icebergs during a Heinrich event (Hemming, 2004), combined with the sustained period of iceberg supply, will enhance the IRD signal from LIS sources at the Goban Spur during Heinrich events. The presence of limited LIS IRD at Porcupine Bank during H2 suggests the Polar Front was a little further south then, and some icebergs from the Hudson Strait managed to remain north of this boundary in crossing the Atlantic (Hemming, 2004). This more southerly position of the Polar Front during Heinrich events is consistent with the Nps data from this and other sites (Scourse *et al.*, 2009; Haapaniemi *et al.*, 2010). Both the IRD and model record are therefore consistent, with the answer to Question 2 being that only exceptional distal ice sheet change affects IRD levels off the BIIS.

Reconciling model and core ocean properties

It has just been seen that the Nps levels (indicative of cold polar waters) off the British margin during Heinrich events are consistent with previous model results for such conditions, where the East Atlantic is colder (Levine and Bigg, 2008; Bigg *et al.*, 2011) and IRD from the LIS can reach the southern section of our study area. Nevertheless, there are some inconsistencies in the background Nps signal found by Scourse *et al.* (2009) along the western European margin. As expected, background levels at Porcupine Bank (50–60%) are lower than those at the more northerly Rosemary Bank (60–80%). Levels at the southernmost site of MD95-2002 are even lower during the first half of our study period (10–40%). These all fit with the model's Polar Front typically being off western Ireland. However, %Nps levels at Goban Spur, off the Isles of Scilly (Fig. 1), are 80–90% for much of our study period; MD95-2002 %Nps levels approach 100% during c. 19–15 ka BP (Scourse *et al.*, 2009). Neither of the more northern cores displayed dramatic increases in %Nps, except during Heinrich events.

It is unlikely these anomalously high %Nps levels, corresponding to particularly cold SSTs, reflect a southward movement of the NAPF, when %Nps values further north remain significantly lower. The most likely explanation for the anomalies is that there is colder water during Marine Isotope Stage (MIS) 2 west of France, with this extending closer to the coast during the last few thousand years of MIS 2. This hypothesis is consistent with both reconstructions of North Atlantic SST and some Palaeoclimate Modelling Project 2 (PMIP2) simulations, while not conflicting with the modelling result here of long-term retention of a region of weak flow and divergence off western Ireland. The GLAMAP 2000 project (Pflaumann *et al.*, 2003; Sarnthein *et al.*, 2003) reconstructed both summer and winter SSTs over the whole Atlantic using a large number of sites, and transfer functions, in part, using %Nps. They found a distinct summer cold core area in the central North Atlantic, off southern Ireland and western France, with locally more sea ice in the winter (Figs. 7 and 8 in Pflaumann *et al.* (2003)), with suspected flows separating around this region, as is consistent with the model circulation here (Fig. 4). Similarly, some, but not all, of the PMIP2 simulations of Li *et al.* (2010) show cold water, and sea ice spreading eastward from the Newfoundland/Labrador Sea area, leading to similar cooling south of Britain, in water not directly connected to the seas off northwestern Ireland and Scotland. The model used here does not show this cold water tongue, as is also the case for half of the PMIP2 simulations, but does support Pflaumann *et al.*'s (2003) hypothesis of a weak, diverging flow west of Ireland. In support of this are also the findings of both the current modelling and Scourse *et al.* (2009), that there is a divide in sourcing IRD throughout non-Heinrich periods of MIS 2 off the Porcupine Bank.

The answer to Question 5 is therefore complex. Changes in climate over time will impact the ocean properties affecting iceberg travel and longevity. However, our current knowledge of the detail of multi-millennial-scale change in these properties, even in the North Atlantic, from both observational and modelling perspectives, is sufficiently limited for it to be problematic to make links between changes in climate, ice sheet and ocean confidently. Despite this, the results described here generate new hypotheses for field and model testing.

Conclusions and consequences

The overall conclusions of the IRD perspective on the peak and deglaciation phases of the last BIIS – that IRD is sourced fairly locally over 31–16 ka BP, except during some Heinrich events in some core locations, and that the likelihood of the mean NAPF separating northward- from southward-moving currents remained around the Porcupine Bank – have been shown to agree with the model simulations. These are less supportive of oscillation of this NAPF boundary during MIS 2 and the end of MIS 3, as they show little movement of this boundary during 'normal' glacial conditions across the study period. Earlier, a possible resolution of the %Nps inconsistencies leading to that Polar Front hypothesis is given, through the inferred presence of a cold tongue extending across the Atlantic south of Britain. Nevertheless, during Heinrich events, which is when Scourse *et al.*, 2009 found %Nps to be greatest at all sites, colder conditions are modelled off western Europe (Levine and Bigg, 2008; Bigg *et al.*, 2011), consistent with both the presence of IRD from the LIS and high levels of Nps. Future work using a fully coupled climate model over this time period would help resolve questions about the stability of the NAPF position.

The details of the IRD–model comparison, and the answers to some of the questions posed earlier, highlight a number of points for future consideration. While for much of the time background IRD levels are stable enough for meaningful comparisons to be made with time-slice models, when IRD peaks occur they tend to be short-lived. Even 1000-year time slices proved difficult for models to accurately reproduce the timing of IRD peaks, with often a 1–2000-year mismatch. Obtaining excellent age control of marine cores is vital in such comparisons. Another question the comparison presents is how ice sheet change is reflected in iceberg, and hence IRD, flux. The case of northwestern Scotland presented this question most clearly. Conceptual models based on ice sheet growth lead to maximum model flux at peak growth, but both Rosemary Bank and Barra Fan suggest peak iceberg flux during the growth phase, and to a greater degree, during the rapid retreat phase of the local continental shelf margin phase of the BIIS. The climate model was able to capture this dual signal at Barra Fan, but not at Rosemary Bank, possibly because the Barra Fan signal was a convolution of signals from the Hebridean and Donegal Ice Streams (Fig. 6). The IRD record suggests iceberg flux was linked to the speed of ice

expansion and retreat. This goes some way to clarifying the question on the indicative meaning of IRD in terms of ice advance or retreat raised in Scourse *et al.* (2009) and repeated here as Question 3.

The question over the extent of the ice sheet over Porcupine Bank (Peters *et al.*, 2016) was not resolved by either analysis. The main long distance iceberg travel from calving in this area is to the south, meaning that neither the model nor the IRD record solves this problem. The model suggests calving to the south is the dominant source region for these far-flung Porcupine Bank icebergs, with most calved from any northern source melting, or grounding, locally. Further resolution of this question will need to rely on sea floor morphological evidence.

Much of the British–Irish margin was well reconstructed by the model, with iceberg origins compatible with the IRD signal. Where the largest discrepancy occurred was to the south, at the Armorican Fan. This highlighted that during rapid retreat of an ice sheet into large enclosed seas, such as the Celtic and Irish Sea, modelling needs to represent such coastline changes more rapidly than is commonly done in time-slice experiments. In that case modelled icebergs would have been released both further north and in enclosed seas where there would be great scope for grounding and melting preventing icebergs from joining the off-shelf southward circulation. In this context, development of an additional IRD depositional model within the iceberg model may help with interpretation of IRD records (e.g. Death *et al.*, 2006), but such a model would still mostly help with interpretation of the background IRD record rather than periods of extreme change, when rapid changes in calving, current rearrangement and local bathymetry exceed most climate models' capabilities. Nevertheless, overall our novel study has shown that high-resolution IRD records can be successfully linked to temporally evolving iceberg trajectory modelling.

Acknowledgements. This research was supported by NERC Large Grant BRITICE-CHRONO NE/J009768/1 to C.D.C., J.D.S. and G.R.B. The University of Exeter allowed some of J.D.S.'s allocation of funding to pay for D.J.W. to work in Sheffield. We would like to thank Dr John Clark of the Department of Computer Science of the University of Sheffield for allowing D.J.W. to go half-time for 6 months while this work was completed through a University of Exeter contract. J.C.E. acknowledges the support of a NERC independent research fellowship (NE/R014574/1). We would like to particularly thank the reviewers for suggesting re-structuring the introductory sections, as well as their suggestions throughout the manuscript.

Data Accessibility

Modelling data are available on request from the authors. IRD data are available as a mix of data in public repositories that issue datasets with DOIs and some on request from the authors.

Supporting information

Additional supporting information may be found in the online version of this article at the publisher's web-site.

Table S1. Mean fluxes for key circulation parameters during a cross-section of the simulations. Means are taken over the last 2 years of the respective simulation (see Fig. S2 for typical variation of some of these). All fluxes are in Sv and air temperature (T) in °C. ST=sub-tropical, SP=sub-polar, SH=Southern Hemisphere. All dates are ka BP.

Figure S1. Variation of orbital parameters over the past 50,000 years. Also shown, in the bottom panel, is the impact on daily July insolation at the top of the atmosphere at 65°N. The period of 31-16 ka BP studied here is marked by the double-headed arrow.

Figure S2. Plots of four major large-scale ocean parameters in the North Atlantic region during the transition from the last 10 years of the spin-up (where the orbital parameters are as for 21 ka BP) through 10 years of forcing with orbital parameters for 31 ka BP. Note that by year 5 of the new state the variables are approaching a new annual cycle equilibrium. This is the largest parameter change relative to the spin-up phase.

Figure S3. The mean 30 m ocean current over the last two years of a selection of simulations is shown for the NE Atlantic (16, 20, 26 and 30 ka BP). Arrow length is linearly related to speed, with longest ~ 30 cms^{-1}. The data is shown over the model x and y grids.

Figure S4. Bar charts of the IRD source variation over time within 2° of the 5 IRD marine cores, using modelled iceberg mass (in Tg) as a proxy. This simulation also includes the Porcupine and Irish Sea modified release sites, shown in Fig. 7. Note that the dotted line is the total BIIS iceberg flux (in km^3 yr^{-1}; see right-hand scale), as reconstructed in Fig. 3. See Figs. 1 and 3 for release sites.

References

Andreassen K, Winsborrow MCM, Bjarnadottir LR *et al.* 2014. Ice stream retreat dynamics inferred from an assemblage of landforms in the northern Barents Sea. *Quaternary Science Reviews* **92**: 246–257.

Andrews JT, Bigg GR, Wilton DJ. 2014. Holocene ice-rafting and sediment transport from the glaciated margin of East Greenland (67-70°N) to the N Iceland shelves: Detecting and modelling changing sediment sources. *Quaternary Science Reviews* **91**: 204–217.

Ballantyne CK, O'Cofaigh C, Coxon P *et al.* 2017. The Last Irish Ice Sheet: extent and chronology. *Advances in Irish Quaternary Studies* **1**: 101–149.

Bamber JL, Riva REM, Vermeersen BLA *et al.* 2009. Reassessment of the potential sea-level rise from a collapse of the West Antarctic Ice Sheet. *Science* **324**: 901–903.

Becquey S, Gersonde R. 2002. Past hydrographic and climatic changes in the SubAntarctic Zone of the South Atlantic – the Pleistocene record from ODP Site 1090. *Palaeogeography, Palaeoclimatology, Palaeoecology* **182**: 221–239.

Berger A. 1988. Milankovitch theory and climate. *Reviews of Geophysics* **26**: 624–657.

Bigg GR, Levine RC, Clark CD *et al.* 2010. Last Glacial ice-rafted debris off south-western Europe: the role of the British-Irish Ice Sheet. *Journal of Quaternary Science* **25**: 689–699.

Bigg GR, Levine RC, Green CJ. 2011. Modelling abrupt glacial North Atlantic freshening: rates of change and their implications for Heinrich events. *Global and Planetary Change* **79**: 176–192.

Callard SL, O'Cofaigh C, Benetti S *et al.* 2018. Extent and retreat history of the Barra Fan Ice Stream offshore western Scotland and northern Ireland during the last glaciations. *Quaternary Science Reviews* **201**: 280–302.

Clark CD, Hughes ALC, Greenwood SL *et al.* 2012. Pattern and timing of retreat of the last British-Irish Ice Sheet. *Quaternary Science Reviews* **44**: 112–146.

Clark CD, Ely JC, Greenwood SL *et al.* 2018. BRITICE Glacial Map, version 2: A map and GIS database of glacial landforms of the last British-Irish Ice Sheet. *Boreas* **47**: 11–27.

Clark CD, Chiverrell RC, O'Cofaig C *et al.* 2020. Foreword: The BRITICE-CHRONO project constraining retreat of the British-Irish Ice Sheet across the marine-to-terrestrial transition. *Journal of Quaternary Science, this volume.*

Death R, Siegert MJ, Bigg GR *et al.* 2006. Modelling iceberg trajectories, sedimentation rates and meltwater input to the ocean from the Eurasian Ice Sheet at the Last Glacial Maximum. *Palaeogeography,Palaeoclimatology, Palaeoecology* **236**: 135–150.

Fanning AF, Weaver AJ. 1996. An atmospheric energy moisture-balance model: climatology, interpentadal climate change and

coupling to an OGCM. *Journal of Geophysical Research - Atmosphere* **101**: 15111–15128.
Gandy N, Gregoire LJ, Ely JC *et al*. 2018. Marine ice sheet instability and ice shelf buttressing of the Minch Ice Stream, northwest Scotland. *Cryosphere* **12**: 3635–3651.
Gowan EJ, Tregoning P, Purcell A *et al*. 2016. ICESHEET 1.0: a program to produce paleo-ice sheet reconstructions with minimal assumptions. *Geoscience Model Development* **9**: 1673–1682.
Green CJ, Bigg GR, Green JAM. 2010. Deep draft icebergs from the Barents Ice Sheet during MIS 6 are consistent with erosional evidence from Lomonosov Ridge, central Arctic. *Geophysical Research Letters* **37**: L2360.
Hall IR, Colmenero-Hidalgo E, Zahn R *et al*. 2011. Centennial- to millennial-scale ice-ocean interactions in the subpolar northeast Atlantic 18-41 kyr ago. *Paleoceanography* **26**: PA2224.
Haapaniemi AI, Scourse JD, Peck VL *et al*. 2010. Source, timing, frequency and flux of ice-rafted detritus to the Northeast Atlantic margin, 30-12 ka: testing the Heinrich precursor hypothesis. *Boreas* **39**: 576–591.
Hemming SR. 2004. Heinrich Events: massive late Pleistocene detritus layers of the North Atlantic and their global climate impact. *Reviews of Geophysics* **42**: RG1005.
Hughes T. 1975. West Antarctic Ice Sheet – instability, disintegration, and initiation. *Reviews of Geophysics* **13**: 502–526.
Knutz PC, Austin WEN, Jones EJW. 2001. Millennial-scale depositional cycles related to British Ice Sheet variability and North Atlantic paleocirculation since 45 kyr BP, Barra Fan, U.K. margin. *Paleoceanography* **16**: 53–64.
Le Brocq AM, Payne AJ, Siegert MJ. 2006. West Antarctic balance calculations: impact of flux-routing algorithm, smoothing algorithm and topography. *Computers and Geosciences* **32**: 1780–1795.
Levine RC, Bigg GR. 2008. The sensitivity of the glacial ocean to Heinrich events from different sources, as modelled by a coupled atmosphere-iceberg-ocean model. *Paleoceanography* **23**: PA4213.
Li C, Battisti DS, Bitz CM. 2010. Can North Atlantic sea ice anomalies account for Dansgaard-Oeschger climate signals? *Journal of Climate* **23**: 5457–5475.
Lüthi D, Le Floch M, Bereiter B *et al*. 2008. High-resolution carbon dioxide concentration record 650,000-800,000 years before present. *Nature* **453**: 379–382.
MacAyeal DR. 1992. Irregular oscillations of the West Antarctic Ice Sheet. *Nature* **359**: 29–32.
Ó Cofaigh C, Weilbach K, Lloyd JM *et al*. 2019. Early deglaciation of the British-Irish Ice Sheet on the Atlantic shelf northwest of Ireland driven by glacioisostatic depression and high relative sea level. *Quaternary Science Reviews* **208**: 76–96.
Patton H, Hubbard A, Andreassen K *et al*. 2016. The build-up, configuration, and dynamical sensitivity of the Eurasian ice-sheet complex to Late Weichselian climatic and oceanic forcing. *Quaternary Science Reviews* **153**: 97–121.
Pearce C, Andrews JT, Bouloubassi I *et al*. 2015. Heinrich 0 on the east Canadian margin: source, distribution, and timing. *Paleoceanography* **30**: 1613–1624.
Peck VL, Hall IR, Zahn R *et al*. 2007. The relationship of Heinrich events and their European precursors over the past 60 ka BP: a multi-proxy ice-rafted debris provenance study in the north east Atlantic. *Quaternary Science Reviews* **26**: 862–875.
Peters JL, Benetti S, Dunlop P *et al*. 2016. Sedimentology and chronology of the advance and retreat of the last British-Irish Ice Sheet on the continental shelf west of Ireland. *Quaternary Science Reviews* **140**: 101–124.
Pflaumann U, Sarnthein M, Chapman M *et al*. 2003. Glacial North Atlantic: sea-surface conditions reconstructed by GLAMAP2000. *Paleoceanography* **18**: 1065.
Rasmussen SO, Bigler M, Blockley SP *et al*. 2014. A stratigraphic framework for abrupt climatic changes during the Last Glacial period based on three synchronized Greenland ice-core records: refining and extending the INTIMATE event stratigraphy. *Quaternary Science Reviews* **106**: 14–28.
Rea B, Newton A, Lamb R *et al*. 2018. Extensive marine-terminating ice sheets in Europe from 2.5 million years ago. *Science Advances* **4**: eaar8327.
Sarnthein M, Gersonde R, Niebler S *et al*. 2003. Overview of glacial Atlantic Ocean Mapping (GLAMAP 2000). *Paleoceanography* **18**: 1030.
Scourse JD, Haapaniemi AI, Colmenero-Hidalgo E *et al*. 2009. Growth, dynamics and deglaciation of the last British-Irish ice sheet: the deep-sea ice-rafted detritus record. *Quaternary Science Reviews* **28**: 3066–3084.
Scourse JD, Saher M, Van Landeghem KJJ *et al*. 2019. Advance and retreat of the marine-terminating Irish Sea Ice Stream into the Celtic Sea during the Last Glacial: timing and maximum extent. *Marine Geology* **412**: 53–68.
Sejrup HP, Clark CD, Hjelstuen BO. 2016. Rapid ice sheet retreat triggered by ice stream debuttressing: Evidence from the North Sea. *Geology* **44**: 355–358.
Smedley RK, Scourse JD, Small D *et al*. 2017. New age constraints for the limit of the British–Irish Ice Sheet on the Isles of Scilly. *Journal of Quaternary Science* **32**: 48–62.
St. John K, Passchier S, Tantillo B *et al*. 2015. Microfeatures of modern sea-ice-rafted sediment and implications for paleo-sea-ice reconstructions. *Annals of Glaciology* **69**: 83–93.
Thomas W. 2014. Research agendas in climate studies: the case of West Antarctic Ice Sheet research. *Climatic Change* **122**: 299–311.
Vettoretti G, Peltier WR. 2013. Last Glacial Maximum ice sheet impacts on North Atlantic climate variability: the importance of the sea ice lid. *Geophysical Research Letters* **40**: 6378–6383.
Wadley MR, Bigg GR. 2000. Implementation of variable time stepping in an ocean general circulation model. *Ocean Modelling* **1**: 71–80.
Wagner TJW, Stern AA, Dell RW *et al*. 2017. On the representation of capsizing in iceberg models. *Ocean Modelling* **117**: 88–96.
Weatherall P, Marks KM, Jakobsson M *et al*. 2015. A new digital bathymetric model of the world's oceans. *Earth and Space Science* **2**: 331–345.
Wilton DJ, Bigg GR, Hanna E. 2015. Modelling twentieth century global ocean circulation and iceberg flux at 48°N: implications for west Greenland iceberg discharge. *Progress in Oceanography* **138**: 194–210.

